



PERGAMON

Available online at [www.sciencedirect.com](http://www.sciencedirect.com)

SCIENCE @ DIRECT®

Electrochimica Acta 48 (2003) 2807–2811

ELECTROCHIMICA  
*Acta*

[www.elsevier.com/locate/electacta](http://www.elsevier.com/locate/electacta)

# Correlation between $\text{AlPO}_4$ nanoparticle coating thickness on $\text{LiCoO}_2$ cathode and thermal stability

Jaephil Cho \*

*Department of Applied Chemistry, Kumoh National Institute of Technology, Gumi, South Korea*

Received 7 February 2003; received in revised form 6 May 2003; accepted 6 May 2003

## Abstract

The thickness of an  $\text{AlPO}_4$  coating significantly affects the thermal stability of a  $\text{LiCoO}_2$  cathode. Increasing the coating thickness leads to not only a decrease in the exothermic reaction between the cathode and the electrolyte but also to an improvement in the cycling performance. A 1 C rate overcharge experiment up to 12 V is a good example of the thermal stability of the cathode in the Li-ion cell. Furthermore, increasing the  $\text{AlPO}_4$  coating thickness results in the lowest cell surface temperature, which is indicative of the degree of heat generation.

© 2003 Elsevier Ltd. All rights reserved.

*Keywords:* Coating thickness; Overcharge; Thermal stability;  $\text{LiCoO}_2$

## 1. Introduction

Commercial Li-ion cells usually operate at a maximum temperature of 60 °C, and protective devices are used to control the cell operating voltage. These protective devices consist of a PTC (positive temperature coefficient) material and protective circuits that block overcharging above 4.35 V, over-discharging below 3 V, and the over-current above 1 C. Despite this protection, many accidents (catch fire and explosion) associated with the cell itself or malfunction of the protective devices have been reported [1]. Such accidents are the result of the thermal runaway of the cell. Thermal runaway occurs when heat generation exceeds heat dissipation because the rate of heat generation increases exponentially with increasing cell temperature, while the rate of heat transfer to a cool environment increases only linearly [2]. Hence, controlling the degree of heat generation is critical to preventing thermal runaway, which is mainly due to the violent exothermic

reaction of  $\text{Li}_x\text{CoO}_2$  with the flammable electrolyte, resulting in oxygen evolution from the cathode [3–7]. In order to minimize the reaction, previous studies have focused on reducing the flammable nature of the electrolytes by adding phosphorus-based additives and co-solvents to the electrolytes or redox shuttle additives [8–12]. However, Cho et al. reported a more fundamental approach to improving the thermal stability of the  $\text{Li}_x\text{CoO}_2$  cathode. They coated the cathode with  $\text{AlPO}_4$  nanoparticles prepared from water [13]. The  $\text{AlPO}_4$  coating improved the thermal stability of the cathode and led to a more uniform coating layer as opposed to using either  $\text{Al}_2\text{O}_3$  or  $\text{ZrO}_2$  coatings derived using the sol–gel method [14–17].

In this paper, the thermal stability of delithiated  $\text{Li}_x\text{CoO}_2$  was investigated by varying the  $\text{AlPO}_4$  coating thickness using differential scanning calorimetry (DSC) and 12 V overcharging experiments. In contrast to the conventional metal oxide sol–gel coating method, this nanoparticle coating led to the easy control of the coating thickness on the cathodes. The 12 V overcharging test was used to characterize the thermal stability of the cathodes in the Li-ion cell.

\* Tel.: +82-54-467-4462; fax: +82-54-467-4477.

E-mail address: [jpcho@kumoh.ac.kr](mailto:jpcho@kumoh.ac.kr) (J. Cho).

## 2. Experimental

The concentration of the  $\text{AlPO}_4$  coating solution was used to control  $\text{AlPO}_4$  coating thickness. 1 g of  $\text{Al}(\text{NO}_3)_3 \cdot 9\text{H}_2\text{O}$  and 0.38 g of  $(\text{NH}_4)_2\text{HPO}_4$  were dissolved slowly in 20 g of water until a white  $\text{AlPO}_4$  nanoparticle suspension was observed (P10). To prepare the P30 scale coating solution, 3 g of  $\text{Al}(\text{NO}_3)_3 \cdot 9\text{H}_2\text{O}$  and 1.14 g of  $(\text{NH}_4)_2\text{HPO}_4$  were dissolved slowly in the same amount of water as P10. Ten grams of  $\text{Al}(\text{NO}_3)_3 \cdot 9\text{H}_2\text{O}$  and 3.8 g of  $(\text{NH}_4)_2\text{HPO}_4$  were used to prepare the P100 scale coating solution. Fifty grams of  $\text{LiCoO}_2$  with an average particle size of 10  $\mu\text{m}$  was added to each coating solution (P10, 30 and 100) and thoroughly mixed for 5 min. The slurry was then dried in an oven at 120  $^\circ\text{C}$  for 6 h and heat-treated in a furnace at 700  $^\circ\text{C}$  for 5 h. For the cycling and DSC tests, a coin-type half-cell with Li metal as an anode was assembled in accordance to the procedure reported in [14]. The half-cells were first cycled for one cycle at a rate of 0.1 rate (= 21 mA/g), followed by 0.5 and 1 C for one cycle and 47 cycles, respectively, between 3 and 4.6 V (The reason for using the stepwise increase in the C rate was to check the capacity drop at each C rate). For the DSC measurements, fresh cells were charged to 4.7 V at a 0.1 C rate, and held at that voltage for 2 h. After disassembling the cells in a globe box, only the cathode composite was obtained from the electrode. Normally the cathode composite contains  $\sim 40$  wt.% of the electrolytes and  $\sim 35$  wt.% cathode material, and only the cathode material was used to measure the heat flow at a heating rate of 3  $^\circ\text{C}/\text{min}$ . Li-ion cells with a 900 mAh standard capacity [cell size:  $3.4 \times 65 \times 50 \text{ mm}^3$  (thickness  $\times$  length  $\times$  width)] were used for the 12 V overcharging test. Either the  $\text{AlPO}_4$  nanoparticle-coated  $\text{LiCoO}_2$  or bare  $\text{LiCoO}_2$ , were used as the cathode. The anode material used was synthetic graphite. The cell surface temperature was monitored using a K-type thermocouple placed on the center of the cell, and the thermocouple was tightly taped using insulating tape. The separator used consisted of PE/PP (polyethylene/polypropylene) (Celgard). The electrolyte used was 1.03 M  $\text{LiPF}_6$  with ethylene carbonate/diethyl carbonate/ethyl–methyl carbonate (EC/DEC/EMC) (30/30/40 vol%). Auger electron spectroscopy (AES) was used to obtain the Al and P elemental distribution near the  $\text{LiCoO}_2$  surface, and its concentration as a function of the depth from the particle surface was measured (the coating depth was estimated from a sputtering rate of 10  $\text{Å}/\text{min}$ , which was calibrated from  $\text{SiO}_2$ ).

Co dissolution from the bare and coated  $\text{LiCoO}_2$  cathodes was measured by inductively coupled plasma-atomic emission spectroscopy (ICP-AES). The electrolytes used to measure the Co dissolution rate were obtained from cycled cells using the centrifugal separation method.

## 3. Results and discussion

The X-ray diffraction patterns of the  $\text{LiCoO}_2$  powders before and after coating were similar, having a hexagonal  $\alpha\text{-NaFeO}_2$  layered structure ( $R\bar{3}m$ ), which is based on a close-packed network of oxygen atoms with alternating Li and Co planes. Fig. 1 shows the AES results of the bare and  $\text{AlPO}_4$ -coated  $\text{LiCoO}_2$  cathodes (P10, 30 and P100) as a function of the depth from the particle surface. The coating thickness was observed to increase with increasing  $\text{AlPO}_4$  concentration, and the P30-coated sample had a coating thickness of  $\sim 200$   $\text{Å}$ , which concurred with the TEM result [13]. The P10 and P100-coated  $\text{LiCoO}_2$  had a coating thickness of  $\sim 60$  and 1000  $\text{Å}$ , respectively. AES analysis of randomly selected points in the P10, P30, P100-coated samples showed that only the Al and P elements were detected in certain thickness from the surface, suggesting a possible complete  $\text{AlPO}_4$  coating layer on the  $\text{LiCoO}_2$  surface. Similarly, TEM analysis of the P30-coated  $\text{LiCoO}_2$  exhibited complete coverage of the coating layer on  $\text{LiCoO}_2$  [13], and indicated  $\text{AlPO}_4$  nanoparticles embedded in the amorphous phase in the coating layer [13]. Detailed studies aimed at elaborating the chemical, microstructural nature of the  $\text{AlPO}_4$  nanoparticles coated on the  $\text{LiCoO}_2$  and the uniformity of the coating layer are currently underway.

Fig. 2 shows the voltage curves, cycle life of the bare and coated cathodes in the coin-type half-cells between 3 and 4.6 V. The small capacity fluctuation during cycling in the P10 and P100-coated cathodes were attributed to the temperature variation in the cycling room. Even though the initial discharge capacities of the samples before or after the coating are similar to each other, the cycle life performance was drastically improved as a result of the coating. A small peak around 4.1 V was observed only in the P30 and P100-coated cathodes, and was reported to be due to a phase transition between the hexagonal and monoclinic phase in  $\text{LiCoO}_2$ . At this

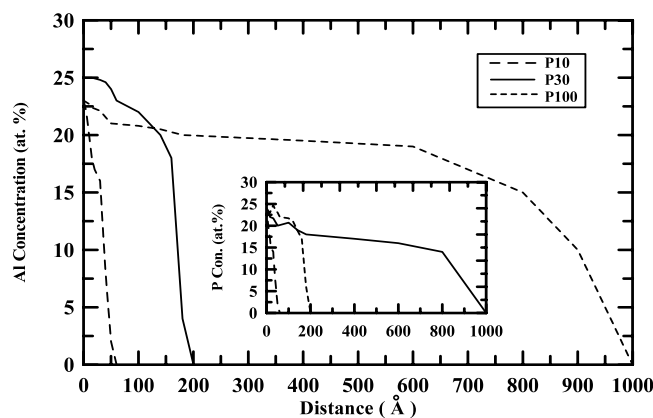


Fig. 1. AES of the aluminum distribution near the particle surface in the P10, 30 and 100-coated  $\text{LiCoO}_2$  powder with distance. The insert shows the AES of phosphorus in the coated particles.

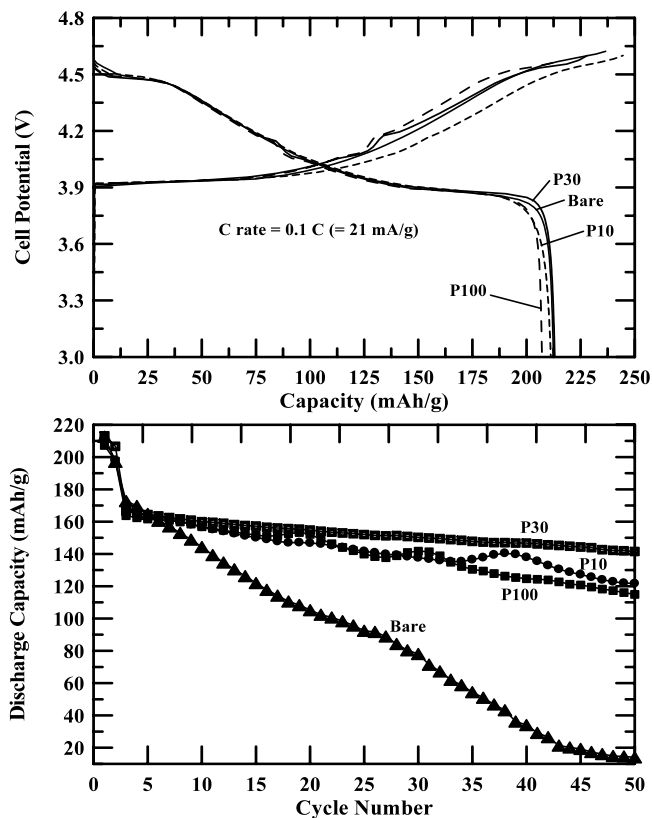


Fig. 2. Plots of (a) the initial charge and discharge curves of the cells containing the bare, and AlPO<sub>4</sub>-coated LiCoO<sub>2</sub> with a different coating thickness at 0.1 C rate (= 21 mA/g) between 4.6 and 3 V and (b) the cycle life results of the cells with the cathodes containing the bare, and AlPO<sub>4</sub>-coated LiCoO<sub>2</sub> with a different coating thickness. The cycle test was carried out initially at 0.1 C for 1 cycle, which was increased to 0.5 and 1 C rates for 1 and 48 cycles, respectively, for a total of 50 cycles.

time, the origin of such an enhanced phase transition of the P30 and P100-coated cathodes to bare cathode is not known. Fig. 3 showed a retention capacity and some Co

dissolution from the bare and coated cathodes after cycling (Co dissolution from the bare and coated electrodes before cycling was ~ 20 ppm). Co dissolution from the coated cathodes after 50 cycles was significantly reduced when compared with the bare sample. Based on these results, the retention capacity appears to correlate with the Co dissolution suppressed by the AlPO<sub>4</sub>-nanoparticle coating layer. Amatucci et al. suggested that the phase change at ~ 4.5 V is sufficiently large to cause mechanical stresses in the grains [18,19]. This electrochemical grinding is coupled with Co dissolution and structural degradation by lithiation/delithiation, resulting in capacity loss. Although Co dissolution of the P100-coated sample after cycling was found to be smaller than that of the P30-coated sample (70 and 160 ppm, respectively), it is believed that the thicker AlPO<sub>4</sub> coating layer with ~ 1000 Å in the P100-coated sample than in the P30-coated sample impeded Li diffusion into the LiCoO<sub>2</sub> particle at higher C rates. However, further studies are needed to correlate the electrochemical properties of the coated samples and the micro-structural differences as a function the coating thickness.

Fig. 4 shows the DSC scans of the Li<sub>x</sub>CoO<sub>2</sub> electrodes at 4.7 V at a heating rate of 3 °C/min. Since *x* in Li<sub>x</sub>CoO<sub>2</sub> is approximately 0.2 at this voltage, and the oxidation state of Co approaches 4+, the Li<sub>x</sub>CoO<sub>2</sub> turns into a very strong oxidant. Hence, any reaction with the electrolyte leads to the violent evolution of oxygen from the cathode. The onset temperature for this oxygen release from bare Li<sub>x</sub>CoO<sub>2</sub> is 187 °C, which accompanies a significant amount of oxygen evolution (substantial amounts of heat generation). The baseline of the bare Li<sub>0.2</sub>CoO<sub>2</sub> was higher than that of the coated cathodes, which may be indicative of the beginning of an exothermic reaction around 100 °C. The quantity oxy-

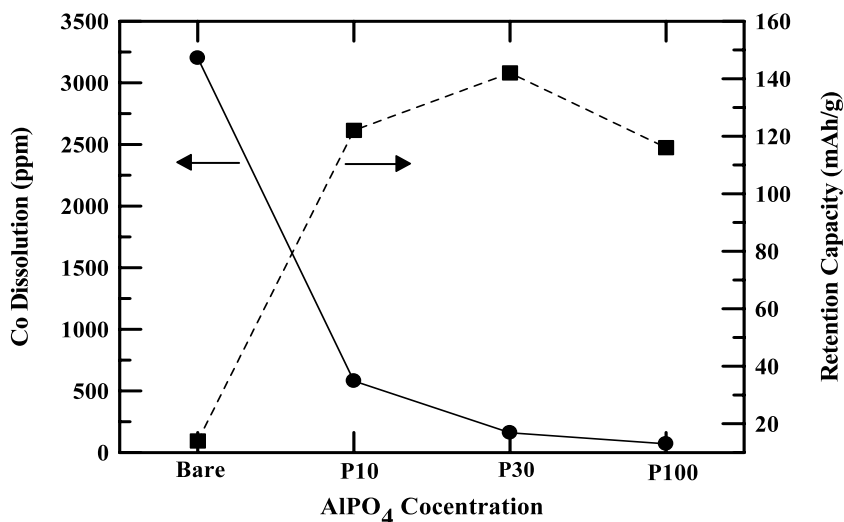


Fig. 3. Plot of the retention capacity and Co dissolution in the bare and AlPO<sub>4</sub>-coated LiCoO<sub>2</sub> cathodes in the coin-type half cells after cycling.

gen evolved can be calculated by integrating the dimensions of the exothermic peaks between 100 and 300 °C. The calculated total heat evolved from the P10, 30, 100-coated LiCoO<sub>2</sub> was estimated to be ~35, ~4 and ~0.1 W/g, respectively, while the bare one was ~320 W/g from 100 to 300 °C. However, the onset temperatures of the AlPO<sub>4</sub>-coated samples increased to 217 °C, which was accompanied by a drastic decrease of oxygen evolution. Even though the initiation temperature of oxygen release remains almost constant, irrespective of the coating thickness, heat generation from the reaction depends strongly on the coating thickness. That is the heat generation rapidly decreased with increasing coating thickness, and it appeared to disappear in the P100-coated sample. This suggests that the AlPO<sub>4</sub> protecting layer is effective in retarding the reaction between the LiCoO<sub>2</sub> and the electrolytes, leading to a decrease in heat generation. Such superior thermal stability over the bare sample is due to the strong covalent bonding of (PO<sub>4</sub>)<sup>3-</sup> with Al [20]. Oxides with (PO<sub>4</sub>)<sup>3-</sup> bonding were reported to have greater thermal stability than λ-MnO<sub>2</sub> even at the fully delithiated state, and MPO<sub>4</sub> (M = Fe and Co) compounds exhibited a weight loss of 1.6% from oxygen evolution while λ-MnO<sub>2</sub> showed a weight loss of 8% when the samples were heated to 500 °C [20,21].

Fig. 5 shows the cell voltage and cell surface temperature profiles of the bare and AlPO<sub>4</sub>-coated cathodes up to 12 V in the Li-ion cells. As the cell voltage was increased to 12 V, the cell temperature was also increased as a result of Joule heat ( $i^2R$ ). In addition, electrolyte decomposition around 5 V (see the plateau in the bare LiCoO<sub>2</sub>) accompanying simultaneous oxygen decomposition from the Li<sub>x</sub>CoO<sub>2</sub> accelerates heat generation, thereby accelerating the temperature rise. At

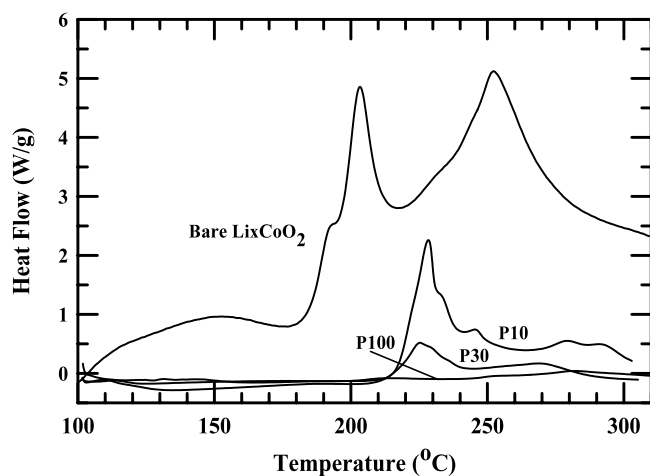


Fig. 4. DSC scans of the charged cathodes containing the bare and AlPO<sub>4</sub>-coated LiCoO<sub>2</sub> with a different coating thickness (P10, 30 and 100) at 4.7 V.

around 6 V, because of the rapid increase in the cell internal resistance, a steep voltage up-surge to 12 V was observed. Even though the cell components, such as the anode and binders also aid the increase in cell temperature, the most contributing factor was the exothermic reaction of the cathode with the electrolytes [3–7]. When the internal temperature exceeds the melting temperature of the separator (<140 °C), the separator shuts down, and temperature begins to decrease as long as an internal short-circuit does not occur. Note that the temperature difference between the internal and the surface of the cell case was approximately 100 °C [3]. All these phenomena can be observed in Fig. 4. However, it should be noted that the electrolyte decomposition plateau at 5 V continues to reduce with increasing coating thickness. Accordingly, such a plateau appears to disappear in the P100-coated sample. Moreover, the cell surface temperature decreases as the coating thickness increases, and the P100-coated-LiCoO<sub>2</sub> showed the lowest surface temperature of 60 °C (cell surface temperature of the bare material shows 100 °C on reaching 12 V). The results suggest that a 5 V plateau plays a key

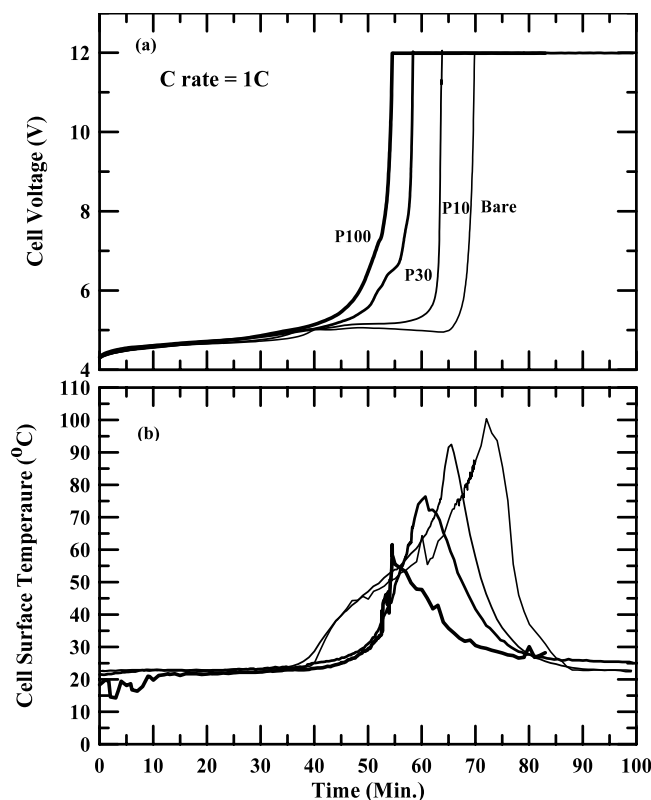


Fig. 5. Plots of (a) the 12 V overcharge curves of the bare and AlPO<sub>4</sub>-coated LiCoO<sub>2</sub> with a different coating thickness in the Li-ion cells. Before overcharging, all the fresh cells were initially charged to 4.2 V at a 1 C rate (=900 mA) and (b) the corresponding cell surface temperature profiles to (a) during overcharge.

role in controlling the heat generation of the cell. This result is well correlated with the DSC result Fig. 4.

#### 4. Conclusions

An  $\text{AlPO}_4$  coating thickness greatly affected the electrochemical properties as well as the thermal stability of  $\text{Li}_x\text{CoO}_2$ . In addition, the exothermic reaction between the cathode and electrolyte was reduced drastically by increasing the coating thickness. Furthermore, the cycling performance was strongly affected by the coating thickness, and the nanoscale ( $\sim 20$  nm) coating layer was believed to be the optimized condition for the cycling performance because the Li diffusivity of the  $\text{LiCoO}_2$  was influenced by the coating thickness. The thermal stability of the charged cathodes was improved with increasing coating thickness; showing not only a rapidly diminished exothermic reaction with the electrolyte, but also an increased onset temperature of oxygen evolution.

#### Acknowledgements

This work was supported by Kumoh National Institute of Technology.

#### References

- [1] Laptop Batteries Are Linked to Fire Risk (New York Times, March 15, 2001); US Consumer Product Safety Commission (<http://www.cpsc.gov/cpscpub>).
- [2] S.C. Levy, P. Bro, Battery Hazards and Accident Prevention, Plenum Press, New York, 1994.
- [3] R.A. Leising, M.J. Palazzo, E.S. Takeuchi, K.J. Takeuchi, J. Electrochem. Soc. 148 (2001) A838.
- [4] H. Maleki, S.A. Hallaj, J.R. Selman, R.B. Dinwiddie, H. Wang, J. Electrochem. Soc. 146 (1999) 947.
- [5] A. Duaquier, F. Disma, T. Bowmer, A.S. Gozdz, G.G. Amatucci, J.-M. Tarascon, J. Electrochem. Soc. 145 (1998) 472.
- [6] H. Maleki, G. Deng, A. Anani, J. Howard, J. Electrochem. Soc. 146 (1999) 3224.
- [7] J.R. Dahn, E.W. Fuller, M. Obrovac, M.U. Von Sacken, Solid State Ionics 69 (1994) 265.
- [8] K. Xu, M.S. Ding, S. Zhang, J. Allen, T.R. Jow, J. Electrochem. Soc. 149 (2002) A622.
- [9] S.C. Narang, S.C. Ventura, B.J. Dougherty, M. Zhao, S. Smedley, G. Koolpe, US Patent #5830660.
- [10] N. Takami, H. Inagaki, H. Ishii, R. Ueno, M. Kanda, IMLB11—Eleventh International Meeting on Lithium Batteries, June 23–28, 2002, Monterey, CA, USA.
- [11] M. Adachi, K. Tanaka, K. Sekai, J. Electrochem. Soc. 4 (1999) 1256.
- [12] X. Wang, E. Yasukawa, S. Kasuya, J. Electrochem. Soc. 148 (2001) A1058.
- [13] J. Cho, Y.-W. Kim, B. Kim, L.-G. Lee, B. Park, Angew. Chem. Int. Ed. 42 (2003) 1618.
- [14] J. Cho, Y.J. Kim, T.-J. Kim, B. Park, Angew. Chem. Int. Ed. 40 (2001) 3367.
- [15] J. Cho, Y.J. Kim, T.-J. Kim, B. Park, Chem. Mater. 13 (2001) 18.
- [16] J. Cho, Y.J. Kim, T.-J. Kim, B. Park, Chem. Mater. 12 (2001) 3788.
- [17] J. Cho, Electrochem. Commun. 5 (2003) 146.
- [18] G.G. Amatucci, J.-M. Tarascon, L.C. Klein, J. Electrochem. Soc. 143 (1996) 1114.
- [19] G.G. Amatucci, J.-M. Tarascon, L.C. Klein, Solid State Ionics 83 (1996) 167.
- [20] A.K. Padhi, K.S. Nanjundaswamy, J.B. Goodenough, J. Electrochem. Soc. 144 (1997) 1188.
- [21] S. Okada, S. Sawa, M. Egashira, J.-I. Yamaki, M. Tabuchi, H. Kageyama, T. Konishi, A. Yoshino, J. Power Sources 97 (2001) 430.